Dynamic fragmentation of a two-dimensional brittle material with quenched disorder

Jan Åström, Markku Kellomäki, and Jussi Timonen
Department of Physics, University of Jyväskylä, P.O. Box 35, FIN-40351 Jyväskylä, Finland
(Received 14 May 1996)

Fragmentation of a two-dimensional brittle material caused by a rapid impact has been analyzed. Computer simulations together with simple arguments are used to obtain a qualitative understanding of crack formation, which is then used to derive an exponential fragment size distribution valid in the large fragment size limit. In the limit of small fragments this distribution is solved numerically, and it is found to obey a scaling law with the exponent -1.5. These results suggest that two different mechanisms are operative in the fragmentation process: branching of propagating cracks determines the small fragment size limit, and merging of the nucleated cracks determines the large size limit. The point of crossover between these two regimes is also found to obey a scaling law. [S1063-651X(97)08204-4]

PACS number(s): 46.10.+z, 46.30.Nz, 05.90.+m, 91.30.−f

During the last decade much effort has been devoted to obtaining a better understanding of the effect of disorder on the fracture of materials [1]. In most cases the model considered has been a lattice network that includes some sort of stochastic disorder. Fracture formation has usually been simulated in these models by repeatedly finding the elastic equilibrium of a strained network, and removing at each step the most strained lattice bond(s) (a ''quasistatic fracture''). In many natural phenomena and technological processes, however, strain is applied so fast that the material will never reach equilibrium. This is true in particular for all types of explosions and rapid impacts. In such cases, elastic or shock waves appear, and damage is caused by material and time-dependent strains (a ''dynamic fracture''). In the quasistatic case a single crack dominates the fracture process [2] and the sample is usually cleaved. In the dynamic case, however, several cracks propagate simultaneously and a fragment size distribution with some rather remarkable features appear [3–9].

The fragment size distribution resulting from a rapid impact has been observed [3–7] to follow a scaling law in the small size limit. The measured scaling exponents range from 1 to 1.7, depending on the shape of the fragmented object [3], and it has been suggested by Oddershede *et al.* [3] that the scaling law is a sign of self-organized criticality. Gilvarry [4], and Klimpel and Austin [10] investigated a model based on the idea of randomly located preexisting defects that act as nucleation centers for cracks. This model reproduces the power law form in the small fragment limit, and it also provides good fits to some experimental data in the large fragment limit. A recent model by Marsili and Zhang also reproduces the power law under some rather general conditions [5]. Similar power laws were found by Hernandez and Herrmann [6] and by Kun and Herrmann [9] using more or less realistic numerical models. A decrease faster than that of the scaling law was observed by Oddershede *et al.* [3] and by Kun and Herrmann [9] in the large fragment limit. The nature of the distribution in this limit, and the crossover between the two regimes has, however, remained unclarified.

In this paper we show that a model based on ideas similar to those of Gilvarry [4] explains well the fragment size distribution of the fractured network in the *large* size limit. In the small size limit we find, as in almost all studies done on fragmentation, that the fragment size distribution follows a scaling law. The scaling exponent, however, is different from the one given by the Gilvarry model. We argue that the fragment size distribution is governed in the small size limit by the dynamics of *single* cracks [11–16], while in the large size limit it is governed by the *merging* of cracks.

The model network we have chosen to analyze is that of a square lattice in which the lattice bonds have the elastic properties of beams with a square cross section w^2, length l, and Young's modulus E. Masses m are placed on each lattice site and the bonds are assumed to be massless [11,12]. The equations of motion can be written [17] in the form $M\ddot{U}=-KU$, where M is a diagonal matrix containing the masses, K is the stiffness matrix, and U is a vector containing the displacements of the nodes. This equation is solved numerically by discretization and iteration of time steps. To avoid nonlinear equations of motion all displacements are assumed to be small in comparison with the length of the bonds. A bond will break when its axial strain exceeds a predefined limit. An elastic wave is applied at the left boundary of the network in such a way that the lattice sites at this boundary are forced to move in the x direction as $A_0\sin^2(\omega t)$ when time t evolves from 0 to π/ω. For $t>\pi/\omega$ these sites are constrained to remain at their original positions. At the right boundary the sites can move without constraints. Periodic boundary conditions are imposed in the y direction.

Disorder is introduced in the network by slightly moving all the lattice sites in a random fashion, and adjusting the lengths of the bonds so that no stress appears. Since no site is moved by more than a half of the length of the lattice bond in any direction, the induced disorder is weak in the sense of Hansen *et al.* [2]. In order to avoid the artifacts caused by a particular direction of wave propagation, two different directions were used in the simulations: parallel to the horizontal bonds (direction I), and diagonally to the bonds (direction II). In contrast with the case of quasistatic load, dynamic fracture is a local phenomenon in the sense that the fracture of a bond will only depend on the stress in the immediate neighborhood of the bond. Consequently, finite size effects should not be as prominent as in the case of static load, and

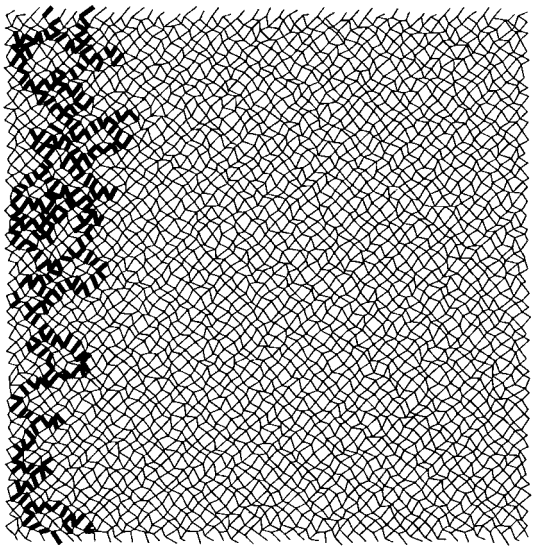

FIG. 1. Fracture paths in a disordered network of size 40×40. The impulse has propagated in direction II. Thick lines indicate broken bonds.

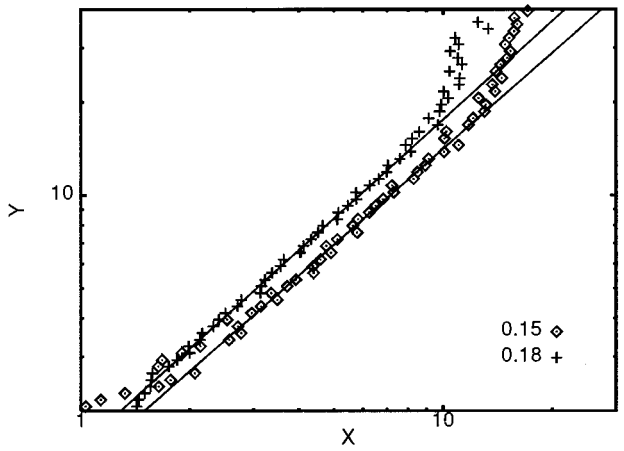

FIG. 2. Y as a function of X for the two propagation directions when only one crack was created. The amplitudes were 0.15 (direction I) and 0.18 (direction II) in lattice units. The fitted lines are given by Eq. (1) with $\zeta=1.03$ and 1.06, respectively. The X and Y axis are in lattice units.

results obtained for a large lattice should hold well in the thermodynamic limit. The absence of large finite size effects was also confirmed by simulations.

In the present model fracture is instantaneous and mechanical contact between fragments is neglected. This means that the amplitude of the elastic signal will decrease drastically when a crack is formed. Consequently, fracture will be located close to the edge of the lattice network (Fig. 1). This type of fracture is called abrasion [7] and in experiments it appears when the energy input is not too far above the limit at which fracture first appears. In order to obtain a qualitative understanding of this type of fracture, we first have to study the dynamics of a single propagating crack. As already mentioned above, we expect that a single crack behaves quite differently for quasistatic fracture and dynamic fracture. We define X and Y to be the width and height, respectively, of the smallest box with sides parallel to the x and y axis, which contains an entire crack. In the dynamic case, fracture depends only on the local stress close to the point where bonds break, which means that we expect X to grow, on the average, proportional to Y. In the quasistatic case, fracture is dominated by stress enhancement at the tip of the crack. This enhancement will increase with the height of the crack, and Y will grow increasingly faster than X. This leads to a power-law relation between X and Y [18,19]

$$Y=aX^{\zeta}, \tag{1}$$

with $\zeta\approx3/2$ and a a positive constant. We have simulated the evolution of single cracks with the dynamic model described above, and the results of these simulations are shown in Fig. 2. The best fits to the data by Eq. (1) give $\zeta\approx1.06$ and 1.03 for direction I and direction II, respectively, as defined above. In other words, the simulations support our assumption that X is proportional to Y.

As illustrated by Fig. 3, a simulated fracture process begins with cracks being nucleated at independently located sites close to the left edge of the network. From these sites cracks begin to propagate and will soon begin to merge. It is also evident from Fig. 3 that merging of cracks causes the height Y of a crack to grow very fast while the width X remains practically unaltered. We thus model the individual cracks as similar cracks initiated at random locations. These cracks are assumed to grow independently of each other such that for each single crack $Y=aX$. When two cracks merge their heights add up (resulting in exponential growth: growth rate is proportional to height), while the total width of the new compound crack is more or less that of its constituents. The growth rate of the height of a crack with this kind of

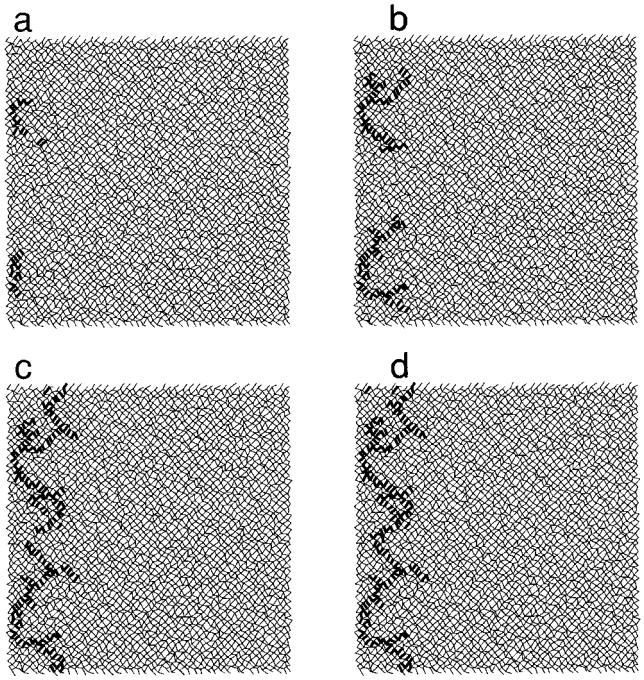

FIG. 3. Snapshot of a fracture process after (a) 1200, (b) 1600, (c) 2000, and (d) 2400 time steps. Notice periodic boundary conditions in the vertical direction. No segments were broken after 2400 time steps.

merging included is therefore influenced by two factors: the growth rate of the height of a single crack, and the height of the growing crack multiplied by the density of cracks. It can thus be expressed in the form

$$\frac{dY}{dX} = a(1 + bY), \tag{2}$$

where b describes the density of initiated cracks. The solution to Eq. (2) is given by

$$Y = \left(\frac{1}{b} + c\right) e^{ab(X-1)} - \frac{1}{b}, \tag{3}$$

where c is the value of Y at $X = 1$.

Evolution of multiple cracks was also simulated in the network model of elastic beams described above, and the results of these simulations together with the corresponding fits by Eq. (3) are shown in Fig. 4. Notice that the same data, for $A = 0.15$ (direction I) and $A = 0.18$ (direction II), appear in Fig. 2 in a log-log scale, while a semilogarithmic scale is used in Fig. 4. In the fits a varied from 1.2 to 1.45 for direction II, and from 0.8 to 1.0 for direction I. This means that the width and height of a single crack grow with approximately the same velocity. As expected, b, which describes the density of initiated cracks was found to increase with the amplitude of the impact: $b = 0.06,0.29,0.42,0.56$ for the amplitudes 0.15,0.18,0.24,0.30, respectively, when waves propagated in direction I, and $b = 0.07,0.15,0.31,0.36$ for $A = 0.18,0.21,0.24,0.27$, respectively, when waves propagated in direction II. Notice that b vanishes at a nonzero amplitude: for small amplitudes only elastic waves appear and no cracks are created. To check if the fitted values of the parameter b really correspond to the amount of initiated cracks, we calculated the number of cracks directly from the simulation results. It is, however, difficult to estimate the exact number of nucleated cracks as propagating cracks sometimes make small jumps and thereby, for a moment, create a new crack at the crack tip [see, e.g., Fig. 3(a), where the upper crack has just made a small jump]. To count the number of nucleated cracks, we therefore estimate the moment in time when almost all cracks are initiated, but crack merging has not yet become dominant. At this moment we then simply count the number of existing cracks. This method will slightly underestimate the number of initiated cracks as the merging of cracks and the creation of new cracks to some extent overlap in time. This effect is strong for high amplitudes when the cracks are nucleated close to each other, which causes cracks to merge quickly. For direction II and networks of size 40×40 we obtained an average of 1.7,5.5,8.9,9.4 cracks for the amplitudes $A = 0.18,0.21,0.24,0.27$, respectively. This should be compared with 2.8,6.0,12.4,14.4 cracks obtained from the fitted b values for the same amplitudes.

Since, for any individual crack, X is proportional to Y, we would expect that for a single propagating crack both of these quantities are linear functions of time. If $X = ct + d$, Eq. (3) can be used to obtain the Y of merging cracks as a nonlinear function of time. In Fig. 5 we show linear fits to simulated $X(t)$ and the resulting fits to the $Y(t)$ as calculated from Eq. (3) with the fitted $X(t)$. It is evident from this figure

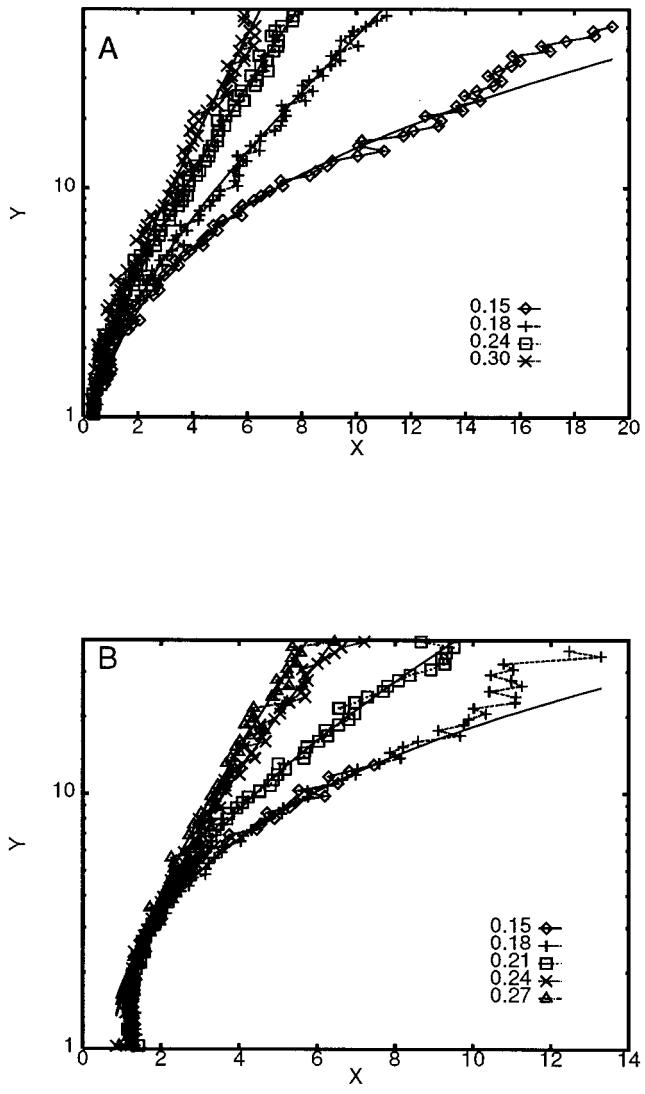

FIG. 4. Y as a function of X for (A) direction I, and (B) direction II. The amplitudes of the impulses were (A) 0.15,0.18,0.21,0.24,0.27, and (B) 0.15,0.18,0.24,0.30. The lines are best fits by Eq. (3). The X and Y axis are in lattice units.

that X grows linearly with time, and that Eq. (3) excellently predicts the time dependence of Y.

The results reported so far prove that the fracture process can be understood in rather simple terms. Cracks originate from randomly located ''weak'' bonds. They propagate independently of each other with, on the average, a constant velocity in the x and y directions until they encounter another crack.

This simple picture can now be used to calculate the experimentally accessible distribution of fragment sizes [3–10]. It is evident from Fig. 3 that large fragments are essentially created between the points where cracks are initiated. Small fragments are created by branching of cracks. To calculate the distribution of the large fragment sizes we again set to b the fraction of lattice bonds on which cracks are simultaneously created. If we further assume that the length of the fragments is proportional to their width, the density $n(r)$ of fragments of linear size r is given by

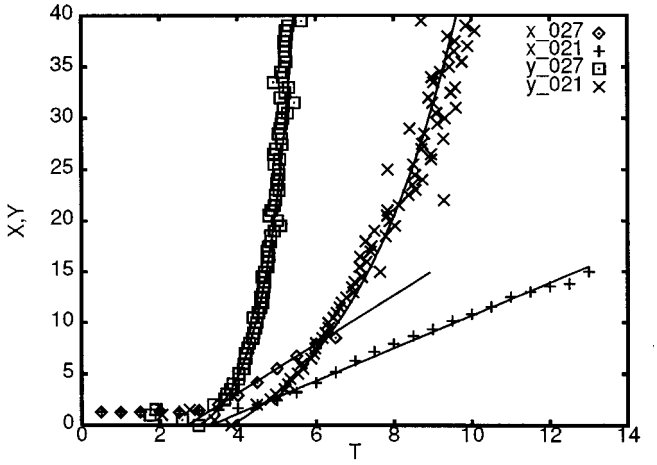

FIG. 5. X and Y as functions of time. Straight lines are fits to simulated X. The other full lines [for $Y(t)$] are given by Eq. (3) with the fitted $X(t)$. Results are shown for amplitudes 0.21 and 0.27.

$$n(r) \propto b(1-b)^{r-1}. \tag{4}$$

This means that the distribution $n(s)$ of fragment areas s for large fragments is given by

$$n(s) \propto \exp[\ln(1-b)(\sqrt{s/p}-1)]/\sqrt{s}, \tag{5}$$

where p is the proportionality factor between the widths and the lengths of the created fragments. From Fig. 3 p can be roughly estimated to be $p \approx 0.3$. The distribution of fragment sizes was simulated by the randomized network of elastic beams, and the resulting cumulative distribution

$$N(s) = \int_s^\infty n(s)ds \propto \exp[\ln(1-b)(\sqrt{s/p}-1)]$$

is shown in Fig. 6 for two different amplitudes. The fitted lines correspond to fractions $b = 0.39$ and $b = 0.31$ of broken bonds for the amplitudes $A = 0.28$ and 0.25, respectively. The

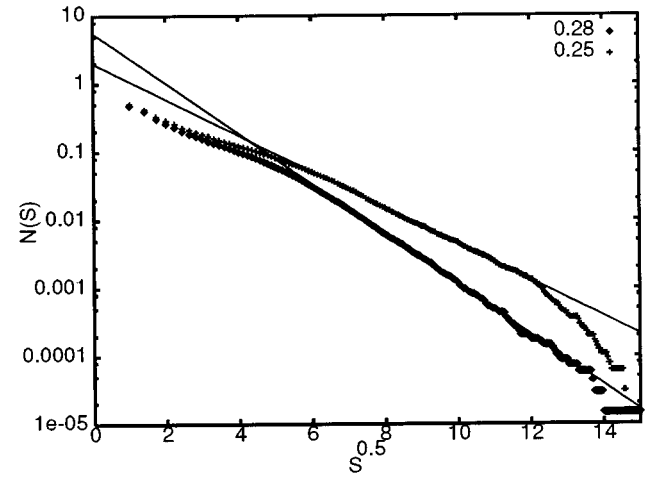

FIG. 6. Semilogarithmic plot of $N(s)$ for amplitudes 0.25 (upper data points) and 0.28 (lower data points). The straight lines are given by Eq. (5) with $b = 0.31$ and 0.39, respectively.

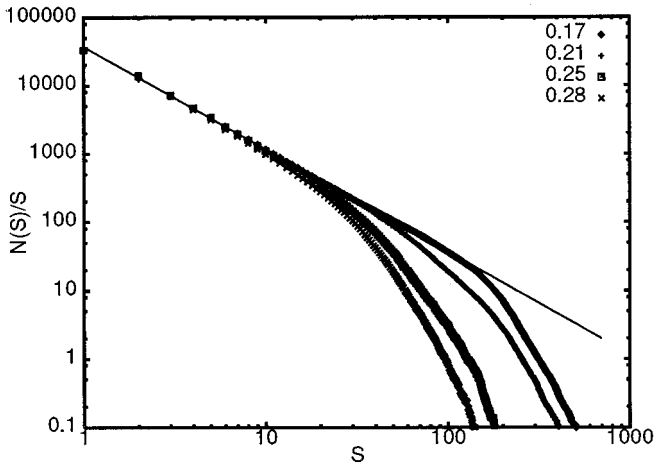

FIG. 7. Log-log plot of $N(s)/s$ for amplitudes 0.17, 0.21, 0.25, and 0.28. The straight line is the function $N(s)/s \propto s^{-1.5}$. The data points deviate later from the line with increasing amplitude.

simulated distributions were found to excellently follow that of Eq. (5), except for small and the very largest fragments. For the largest fragments the deviation is obviously due to finite size effects. It has been observed [3–10] in the small size limit in particular that fragment size distributions universally follow a scaling law. In this limit, Eq. (5) gives $n(s) \propto s^{-0.5}$. By plotting the data of Fig. 6 on a log-log scale in Fig. 7 it becomes evident that

$$n(s) \propto s^{-1.5} \tag{6}$$

in the small size limit, which is clearly different from Eq. (5). This discrepancy means that the mechanism behind the distribution Eq. (5), which seems to excellently explain the simulated distribution of large size fragments, does not dominate the production of small size fragments. So there must be some other mechanism that governs the formation of these small fragments. An obvious mechanism for this task is the branching of propagating cracks (hints of this can be seen in Fig. 3). It is also interesting to notice that -1.5 is the

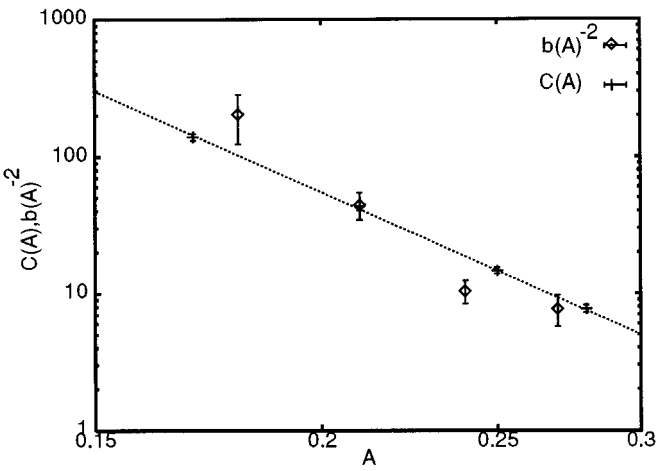

FIG. 8. Log-log plot of $C(A)$ for the data of Fig. 7 compared with $b^{-2}(A)$. The straight line is $C(A) \propto A^{-5.92}$.

exponent found by Hernandez and Herrmann [6] in their ''model B'' with the ''relaxed stopping'' criterion.

Furthermore, it is also evident from Fig. 7 that there must be two different mechanisms that are operative in the small size and in the large size limit, respectively, of $n(s)$. In the first limit $n(s)$ is independent of the amplitude of the impulse while it is amplitude dependent in the second limit. (Notice that we have not normalized the distributions in Fig. 7. They show the actual number of fragments created in the simulations.) A reasonable explanation for the two different mechanisms is, as already pointed out, that fragments created by merging of cracks dominate the large size limit of $n(s)$, while those created by branching of cracks dominate the small size limit. In this case the size and abundance of the large fragments would strongly depend on the amplitude through the parameter b in Eqs. (5) and (3), while small fragments would not depend on the amplitude as the branches are created only after the main impulse has passed by. As a consequence, the power-law distribution Eq. (6) is expected to be valid for fragments with linear size smaller than the average distance between nucleated cracks $(1/b)$, while Eq. (5) should be valid for fragments larger than $1/b$. The fragment area at the point of crossover $[C(A)]$ between the two regimes obtained from simulations is compared with $1/b^2(A)$ in Fig. 8. The data presented in this figure clearly support the above explanation. It is also interesting to notice that the $C(A)$ of Fig. 8, which gives the scaling range, also satisfies a power law: $C(A)=A^{-5.92}$.

In summary, we have demonstrated that the basic features, apart from branching, of the dynamic crack formation can be understood within a simple model. The growth of cracks is in the direction of propagation dominated by merging of cracks, and this causes the length of a crack to grow exponentially with time. The growth of the width of the cracks is linear with time. The fragment size distribution follows a scaling law in the small size limit, and there is a crossover to an exponential behavior in the large size limit. The explanation for this behavior seems to be that large fragments are created through merging of initially nucleated cracks, while small fragments are created through branching processes. The size of the scaling regime is given by a power law in the amplitude of the impact.

[1] *Statistical Models for the Fracture of Disordered Media*, edited by H.J. Herrmann and S. Roux (North-Holland, Amsterdam, 1990).
[2] A. Hansen, E.L. Hindrichsen, and S. Roux, Phys. Rev. B **43**, 665 (1991).
[3] L. Oddershede, P. Dimon, and J. Bohr, Phys. Rev. Lett. **71**, 3107 (1993).
[4] J.J. Gilvarry, J. Appl. Phys. **32**, 391 (1961).
[5] M. Marsili and Y.-C. Zhang (unpublished).
[6] G. Hernandez and H.J. Herrmann, Physica A **215**, 420 (1995).
[7] S. Redner, in *Statistical Models for the Fracture of Disordered Media* (Ref. [1]).
[8] Z. Cheng and S. Redner, J. Phys. A **23**, 1233 (1990).
[9] F. Kun and H.J. Herrmann, Int. J. Mod. Phys. C **7**, 837 (1996).
[10] R.R. Klimpel and L.G. Austin, Trans. AIME/SME **232**, 88 (1965).
[11] P. Heino and K. Kaski, Phys. Rev. B **54**, 6150 (1996).
[12] M. Marder and X. Liu, Phys. Rev. Lett. **71**, 2417 (1993).
[13] E. Sharon, S.P. Gross, and J. Fineberg, Phys. Rev. Lett. **74**, 5096 (1995).
[14] J. Fineberg, S.P. Gross, M. Marder, and H.L. Swinney, Phys. Rev. Lett. **67**, 457 (1992).
[15] S.P. Gross, W.D. McCormick, M. Marder, and H.L. Swinney, Phys. Rev. Lett. **71**, 3162 (1993).
[16] F. Abraham, D. Brodbeck, R.A. Rafey, and W.E. Rudge, Phys. Rev. Lett. **73**, 271 (1994).
[17] The method is similar to that used in the time-dependent finite element method.
[18] A. Hansen, E.L. Hindrichsen, and S. Roux, Phys. Rev. Lett. **66**, 2476 (1991).
[19] K.J. Måløy, A. Hansen, E.L. Hindrichsen, and S. Roux, Phys. Rev. Lett. **68**, 213 (1992).